Temperature dependence of structure of liquid tin studied by a first-principles molecular-dynamics simulation

S. Munejiri,[1] , Y. Senda[†,2], F. Shimojo[†,3], K. Hoshino[†] and T. Itami[‡]

NASDA, Tsukuba 305-8505, Japan
† *Hiroshima University, Higashi-Hiroshima 739-8521, Japan*
‡ *Division of Chemistry, Graduate School of Science, Hokkaido Univ., Sapporo 060-0810, Japan*

Abstract The temperature dependence of the structure of liquid tin was studied from 773 to 1873 K by a first-principles molecular-dynamics simulation. The calculated results were discussed with the neutron scattering experiments.

1 Introduction

It is well known that the structure factor, $S(Q)$, of liquid tin near the melting point has a shoulder on the high-Q side of the main peak [1, 2]. This shoulder has been explained by the difference between the effective core radius and the wavelength of the Friedel oscillation in the interatomic pair potential[3] or the existence of the covalent bonds even in the liquid metal [4]. It is an interesting issue that how such complex structures change with variation of temperature. To clarify this issue our project team carried out a neutron scattering experiment and a first-principles molecular-dynamics (FPMD) simulation for a wide range of temperature [5, 6].

In this paper, we study the temperature dependence of the structure of liquid tin by the FPMD simulations.

2 Method of Calculation

Our method of the FPMD calculation is based on the density functional theory with the local density approximation[7]. For the interaction between the valence electrons and the ion, we employ the norm-conserving pseudopotential by Troullier and Martins[8], which is derived from the calculation of the atomic electron configuration $5s^2\ 5p^2\ 5d^0$. The electronic wave functions are expanded in terms of a plane wave basis set with a cutoff energy of 11 Ryd. The Γ point is used to sample the Brillouin zone of the supercell. The Kohn-Sham energy functional is minimized by the preconditioned conjugate-gradient method[9, 10, 11]. Then the forces on the ions are calculated using the Hellmann-Feynman theorem. The MD simulations are carried out with 64 atoms in a cubic supercell from 773 to 1873 K. For the density of the system, the experimental data[12] are used. The mass and the number densities of the system are $6.82 \sim 6.15$ g cm $^{-3}$ and $0.0346 \sim 0.0312$ Å^{-3}, respectively. The lengths of the side of the cubic supercells are $12.3 \sim 12.7$ Å. The

[1]Present address: Hijiyama Univ. Hiroshima, 732-8509, Japan
[2]Present address: Kanazawa Univ. Kanazawa, 920-1192, Japan
[3]Present address: Kumamoto Univ. Kumamoto, 860-8555, Japan

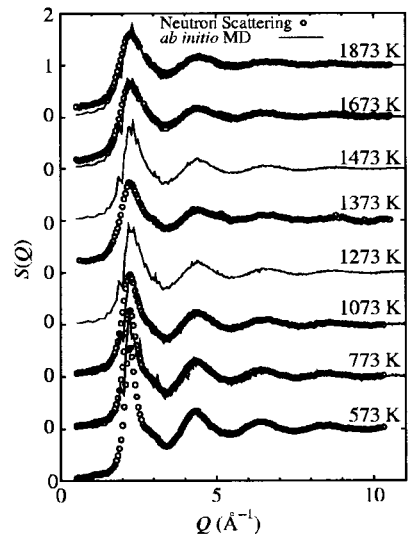

Figure 1. Structure factors, $S(Q)$'s, of liquid tin at the temperatures from 573 to 1873 K.

constant temperature simulations are performed using the Nosé-Hoover thermostat[13, 14] for 10000 steps with the time steps 150 $\sim$ 200 a.u.(3.6 $\sim$ 4.8 fs). The simulations were performed on the supercomputer VPP500 at the Center for Promotion of Computational Science and Engineering of JAERI and the workstations at National Space Development Agency of Japan.

3 Results and Discussion

The structure factors, $S(Q)$'s, and the radial distribution functions, $g(r)$'s, obtained in the present study are shown in figures 1 and 2, respectively. The lines and the circles show the results obtained from the FPMD simulation and from the neutron scattering, respectively. The calculated results are in excellent agreement with the experiments. The shoulder around $Q = 2.8$ Å^{-1} is reproduced at low temperatures. With increasing temperature, the first peak becomes lower and broader and the shoulder seems to disappear. The characteristic features in $g(r)$ are the flatness and the large values in the region between the first and the second peaks compared with those of simple liquids. With increasing temperature, though the height of the first peak in $g(r)$ becomes lower, the values of $g(r)$ in this flat region are almost unchanged. Similarly, the values of $S(Q)$ around the shoulder stay almost constant with varying temperature and the shape of the first peak of $S(Q)$ is asymmetric even at the highest temperature of 1873 K.

To study the microscopic structure more in detail, a three-body angle distribution function $g^{(3)}(\theta, r_c)$ was calculated from the atomic configuration and the results at 773 and 1873 K are shown in figure 3. The three-body angle is formed by a pair of vectors drawn from a reference atom to any other two atoms within a cutoff radius r_c (see the inset in figure 3). When the cutoff radius r_c is 3.4 Å, which is longer than the average nearest neighbor distance, $g^{(3)}(\theta, r_c)$ shows a clear peak centered at 60°. When an interatomic interaction is isotropic and the atoms are in closed-packed, $g^{(3)}(\theta, r_c)$ should show the peak around 60°. Therefore this peak indicates a typical structure in a simple liquid. With decreasing

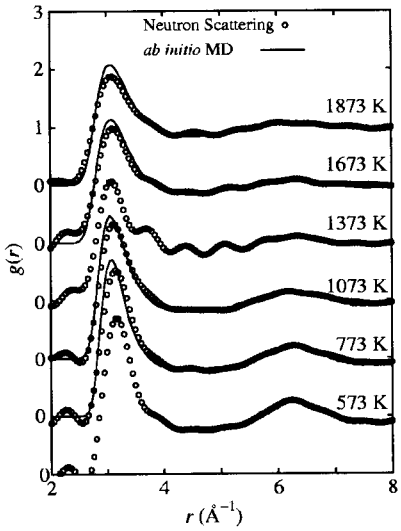

Figure 2. Radial distribution functions, $g(r)$'s, of liquid tin at the temperatures from 573 to 1873 K.

the cutoff radius r_c, the peak at 60° disappears and $g^{(3)}(\theta, r_c)$ shows only single broad peak distributed near 100° close to the tetrahedral bond angle of 109°. This peak suggests that there are complex local structures due to anisotropic interactions in liquid tin. With increasing temperature, $g^{(3)}(\theta, r_c)$ becomes broad for r_c = 3.1 and 3.4 Å, while that for r_c = 3.0 Å is almost unchanged. This means that the short-range structure within 3 Å does not so much depend on the temperature in the temperature range of the present study.

It is well known that $S(Q)$'s of liquid silicon and germanium also have the shoulder on the high-Q side of the first peak[1] and at the same time their $g^{(3)}(\theta, r_c)$'s show the peak around 100°[10, 15, 16, 17]. On the other hand, for liquid lead, which is also the group IV element, there is no shoulder in $S(Q)$ and no peak around 100° in its $g^{(3)}(\theta, r_c)$[1, 6, 18]. These facts imply that the shoulder in $S(Q)$ is related to the short-range structure making the peak around 100° in $g^{(3)}(\theta, r_c)$. From the results of $g(r)$, $S(Q)$ and $g^{(3)}(\theta, r_c)$ in the present study, it is considered that the shoulder in $S(Q)$ of liquid tin does not disappear but is merely covered by the broadened first peak at high temperatures.

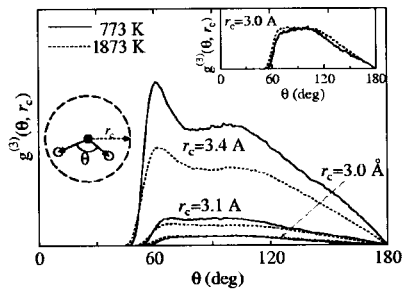

Figure 3. Three-body angle distribution functions, $g^{(3)}(\theta, r_c)$'s , at 773 K and 1873 K.

The coordination number, n, is usually calculated by the integration of $g(r)$. For the liquid tin, however, since the position of the first minimum is not clear and the first peak is asymmetric, the definition of the coordination number is difficult. Therefore the distribution of the coordination number with the cutoff length r_c was investigated and the results at 773 K and 1873 K are shown in figure 4. Though, from the structure in the solid state with $n = 4$ and from the bond angle distribution function for $r_c = 3.0$ Å, the existence of the tetrahederal structure is implied, few four-fold structures are found in $d(n)$ within $r_c = 3.0$ Å. When r_c is fixed, the average coordination number decreases with increasing temperature for $r_c \geq 3.1$ Å. For $r_c = 3.0$ Å, however, $d(n)$ is almost unchanged with changing temperature. This means that the short-range structure does not so much depend on the temperature.

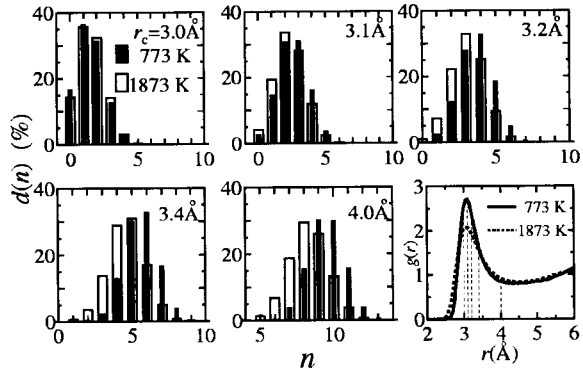

Figure 4. Distributions of the coordination number $d(n)$ of liquid tin at 773 K and 1873 K. The radial distribution functions at the same temperatures are also shown.

From the present FPMD simulations, the information of microscopic atomic motion can be obtained. The mean square displacement (MSD) of atoms is shown in figure 5. Three regions can be seen in this figure, the free particle behavior of parabolic time dependence ($t < 0.1 \sim 0.2$ ps), the region of linear time dependence of the diffusion law ($t >\sim 0.3$ ps) and the transition region between them. Figure 6 shows the normalized form of the velocity auto correlation function (VAF), $Z(t)$. The normalized VAF, $Z(t)/Z(0)$, decreases rapidly with the progress of time and then the oscillatory negative regions can be seen below 1273 K. However, over 1473 K, the normalized VAF indicates no negative regions though oscillatory behaviors themselves can be seen. These facts indicate that the back scattering effect or cage effect is present clearly at lower temperatures. However, at high temperatures, such an effect is weaker or absent though the interaction with surrounding atoms itself still works judging from the existence of oscillatory behavior. Such a complicated interaction can be seen also from the complicated spectrum of the VAF, $\tilde{Z}(\omega)$, shown in figure 7.

The self-diffusion coefficients, D's, were calculated both from the MSD of atoms and from the VAF. Since the simulations were carried out for long time, 36~48 ps (10000 step), the results obtained from the MSD and the VAF are in good agreement with each other. The D values of our present simulation, shown in figure 8, are about half of the experimental D obtained under microgravity [19, 20, 21] in spite of the fact that the calculated structure factors, $S(Q)$'s, are in excellent agreement with the experimental $S(Q)$'s. One of problems

in the present simulation is the small system size in the FPMD simulation. To check the size dependence of D, we have performed the FPMD simulation for liquid Sn at 773 K using a larger system composed of 125 atoms for 800 time steps. Though the statistical average for D in this short time simulation is not so good, the result of D is about thirty percent larger than that calculated in the system of 64 atoms with the same time steps. One of the other factors for the improvement of the calculated value of D may be the pressure of the system in the simulation. In our MD simulation the experimental value of the density [12] was used at each temperature. When the density and the temperature are fixed, the pressure is uniquely determined in the thermodynamics. However, since our simulation was carried out under constant number of atoms, constant temperature and constant volume (NVT ensemble) in the small systems, the pressure may not be the same as the macroscopic one.

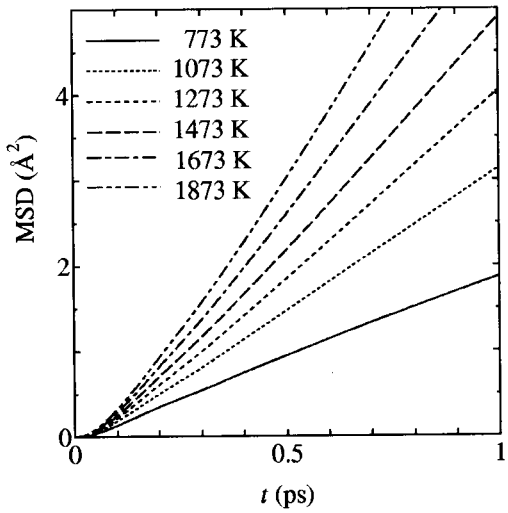

Figure 5. The variation of the mean square displacement (MSD) with time, t, for liquid tin from 773 K to 1873 K.

4 Summary

Temperature dependence of structure of liquid tin was investigated by the FPMD simulation. A shoulder on the high-Q side of the first peak of $S(Q)$ can be seen at low temperatures. Since even at 1873 K the main peak is asymmetric, such a shoulder may be present though it becomes unclear in the change of overall pattern of $S(Q)$. A broad peak around 100° in the three body distribution function was observed up to 1873 K. The coordination number with cutoff radius of 3.0 Å does not change with the increase of temperature from 773 K to 1873 K though it decreases with the increase of temperature in the case of larger cutoff radius. These features indicate that some local structure which is produced by many body force may persist even at high temperature in the liquid tin.

Acknowledgement

We are grateful to Prof. S. Takeda and Dr. Y. Kawakita for valuable suggestions and discussions.

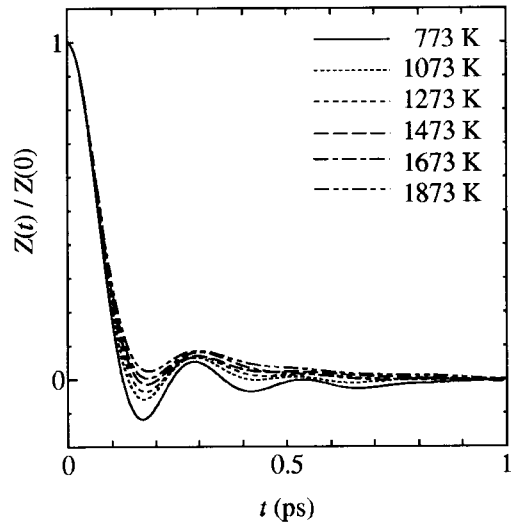

Figure 6. The variation of the velocity autocorrelation function (VAF) with time, t, for liquid tin from 773 K to 1873 K ($Z(t)$: VAF at time t).

References

1. Y. Waseda, *The Structure of Non-Crystalline Materials, Liquid and Amorphous Solid* (McGraw-Hill, New York, 1980).
2. S. Takeda, S. Tamaki and Y. Waseda: *J. Phys. Soc. Jpn.* **53** (1984) 3447.
3. Ya, Chushak, J. Hafner and G. Kahl: *Phys. Chem. Liq.* **29**, (1995) 159.
4. N. W. Ashcroft: *Nuovo Cimento* D **14**, (1984) 2259.
5. S. Munejiri, T. Masaki, Y. Ishii, T. Kamiyama, Y. Senda, F. Shimojo, K. Hoshino, and T. Itami: *J. Phys. Soc. Jpn. Suppl.* A 70,(2001) 268.
6. T. Itami, S. Munejiri, T. Masaki, H. Aoki, Y. Ishii, T. Kamiyama, Y. Senda, F. Shimojo and K.Hoshino: *Phys. Rev.* B (2003) in press.
7. D. M. Ceperley and B. J. Alder: *Phys. Rev. Lett.* **45** (1980) 566; J. P. Perdew and A. Zunger: *Phys. Rev.* B **23** (1981) 5048.
8. N. Troullier and L. L. Martines: *Phys. Rev.* B **43** (1991) 1993.
9. M. P. Teter, M. C. Payne and D. C. Allan: *Phys. Rev.* B **40** (1989) 12255.
10. G. Kresse and J. Hafner: *Phys. Rev.* B **49** (1994) 14251.
11. F. Shimojo, Y. Zempo, K. Hoshino and M. Watabe: *Phys. Rev.* B **52** (1995) 9320.
12. P. M. Nasch and S. G. Steinemann: *Phys. Chem. Liq.* (UK) **29** (1995) 43.
13. S. Nosé: *Mol. Phys.* **52** (1984) 255.
14. W. G. Hoover: *Phys. Rev.* A **31** (1985) 1695.
15. I. Štich, R. Car and M. Parrinello: *Phys. Rev. Lett.* B **63** (1989) 2240; I. Štich, R. Car and M. Parrinello: *Phys. Rev.* B **44** (1991) 4262.
16. C. Z. Wang, C. T. Chan and K. M. Ho: *Phys. Rev.* B **45** (1992) 12227.
17. R. V. Kulkarni, W. G. Aulbur and D. Stroud: *Phys. Rev.* B **55** (1997) 6896.
18. Y. Senda, F. Shimojo and K. Hoshino: *J. Phys.: Condens. Matter* **11** (1999) 2199 and private communication.
19. G. Frohberg, K. H. Kraatz and H. Weber: *Proc. 6th Europ. Symp. on Material Sciences under microgravity conditions, Bordeaux, 1986*, p. 2.
20. T. Itami *et al.*: it J. Jpn. Soc. Microgravity Appl. **15** (1998) 225; S. Yoda *et al.*: *J. Jpn. Soc. Microgravity Appl.* **15**, Supplement II (1998) 343.
21. C. H. Ma and R. A. Swallin: *J. Chem. Phys.* **46** (1962) 3014

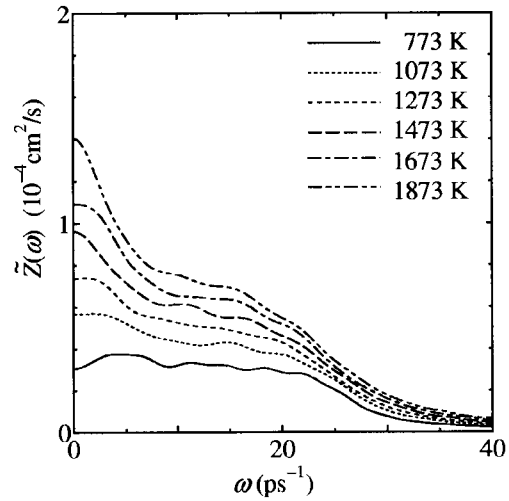

Figure 7. The variation of the spectrum of the VAF, $\tilde{Z}(\omega)$, for liquid tin from 773 K to 1873 K.

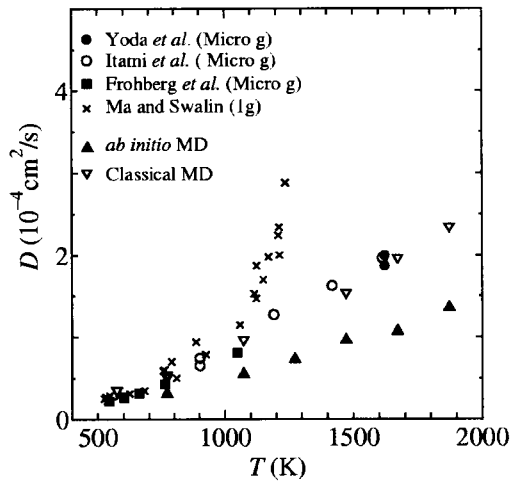

Figure 8. The self-diffusion coefficient ,D , of liquid tin.